24th INTERNATIONAL CONGRESS ON SOUND AND VIBRATION
23–27 July 2017, London

ICSV24
23-27JULY 2017
LONDON CALLING

LINEAR AND NONLINEAR STABILITY PREDICTIONS FOR A DOMESTIC BOILER WITH A HEAT EXCHANGER FOR PASSIVE INSTABILITY CONTROL

Aswathy Surendran and Maria A. Heckl
School of Chemical and Physical Sciences, Keele University, Staffordshire, ST55BG, UK
email: a.surendran@keele.ac.uk

In this study, we investigate the stability behaviour of a domestic boiler system, when the heat absorption rate at the heat exchanger (hex) varies with the mean flow velocity and with the amplitude of velocity fluctuations upstream of the hex. The domestic boiler system is modelled as a 1D quarter-wave resonator (open at one end and closed at the other). The hex is placed near the closed end, and the flame is upstream of the hex. The flame is modelled as a compact heat source, assumed to follow a basic $n-\tau$ law. The heat absorption rates at the hex are treated as amplitude-dependent and are calculated in two ways: (1) computed from numerical simulations and (2) from an empirical correlation based on King's law for the heat release rate of a hot wire. The stability analysis is done in the frequency domain, and the stability predictions are carried out using the classical eigenvalue method.

Keywords: heat exchanger, amplitude-dependent heat absorption rate, instability control

1. Introduction

One of the major concerns in the operability of power generation systems is their susceptibility to combustion instabilities. In the present work, we focus our attention on the thermoacoustic instabilities in small and compact power generation units, which have both the heat source and the heat exchanger (hex) housed in the combustion chamber. A common example of such a unit is a domestic boiler. The stability behaviour is not just determined by the flame (a heat *source*), but also by the hex, which acts as a heat *sink* as well as an acoustic scatterer. In works dating back to the 1850s, Bosscha [1] and Riess [2] discussed the influence of a heat sink on the stability of a Rijke tube. They observed loud pressure oscillations when a cold wire gauze (i.e., a heat sink) was placed at the upper extremity of a Rijke tube and exposed to a hot cross-flow.

Surendran et al. [3, 4] have shown the passive control capability of cavity-backed heat exchangers with bias-flow, by appropriately varying the cavity length and the mean bias-flow. They looked at the linear stability of a quarter-wave resonator with a heat source near the open end and a heat exchanger, placed near the closed end of the resonator. The present study is an extension of the work by Surendran et al. [4], in that we now consider a hex, which responds to velocity fluctuations with an *amplitude-dependent* heat absorption rate. Any other amplitude-dependence is ignored, i.e., we assume that the amplitude of the velocity fluctuations does not affect the $n-\tau$ law for the heat source or the acoustic scattering at the hex tube row. In other words, only the heat absorption rate at the heat sink is treated as nonlinear. We will evaluate the heat absorption rates through numerical simulations as well as by using an empirical formula given in Heckl [5].

2. Description of system

The configuration studied is similar to the one given in [4]. It consists of a quarter-wave resonator with both heat source (flame) as well as heat sink (hex) as shown in Fig. 1. The upstream end, $x = 0$, is open and the corresponding reflection coefficient is given by $R_0 = -1$. The heat source is located at a distance l_f from the upstream end and the hex is located at $x = L$. The distance between the hex tube row and the closed downstream end of the resonator, referred to as cavity length, is denoted by l_c. The heat source and the hex divide the resonator into a cold upstream region (Region 1), hot intermediate region (Region 2) and a relatively (with respect to Region 2) cold downstream region (Region 4).

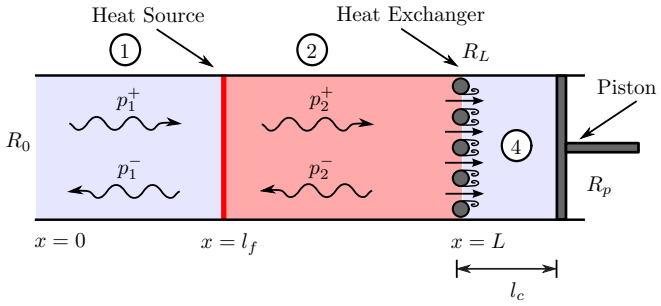

Figure 1: Schematic of the combustion system being studied.

The acoustic waves are assumed to be one-dimensional and propagating perpendicular to the hex tubes (normal incidence). The speeds of sound ($c_{1,2,4}$) and mean temperatures ($\bar{T}_{1,2,4}$) are uniform within each region, where $\bar{T}_1 < \bar{T}_4 < \bar{T}_2$ and subsequently $c_1 < c_4 < c_2$. The acoustic pressure and velocity fields within the combustion system are denoted as

$$p_r(x) = p_r^+ + p_r^- = A_r e^{ik_r(x-l_f)} + B_r e^{-ik_r(x-l_f)} \,, \tag{1}$$

$$u_r(x) = u_r^+ + u_r^- = \frac{1}{\rho_r c_r} \left\{ p_r^+ - p_r^- \right\} \,, \tag{2}$$

where p^+ and p^- are the forward and backward travelling pressure waves respectively, A and B are the pressure amplitudes and u^+ and u^- are the acoustic velocities corresponding to p^+ and p^- respectively. The subscript 'r' denotes the region within the combustor, ω is the frequency of the acoustic wave, c_r is the speed of sound inside the resonator, $k_r = \omega/c_r$ is the wavenumber and ρ_r is the density of the medium within the resonator. The factor $e^{-i\omega t}$ is omitted throughout the analysis.

The heat source is assumed to be compact, planar and confined to an infinitesimally thin region at $x = l_f$. The heat release rate fluctuation ($\hat{Q}_f$) is assumed to follow the time-lag law, and to depend on the velocity fluctuations at the location, l_f, with a time-lag τ and an interaction index n i.e.,

$$\hat{Q}_f(x,\omega) = n\, u_1(x) e^{i\omega\tau} \delta\left(x - l_f\right) \,. \tag{3}$$

With Eq. (2), $\hat{Q}_f(x,\omega)$ can be expressed in terms of the acoustic pressure as

$$\hat{Q}_f\left(x,\omega\right)|_{x=l_f} = n\, e^{i\omega\tau} \frac{\left(p_1^+ - p_1^-\right)}{\rho_1 c_1} \,. \tag{4}$$

Across the heat source, at $x = l_f$, we assume continuity of pressure,

$$p_1^+ + p_1^- = p_2^+ + p_2^- \,, \tag{5}$$

and a velocity jump generated by the heat source [6]

$$\left(u_2^+ + u_2^-\right) - \left(u_1^+ + u_1^-\right) = \frac{(\gamma - 1)}{S\rho_1 c_1^2}\hat{Q}_f \,, \tag{6}$$

where S is the cross-sectional area of the duct and γ is the ratio of the specific heat capacities.

3. Heat exchanger modelling

The hex at $x = L$ acts as both heat sink and acoustic scatterer. These two physical processes are modelled and treated as individual processes, separated by an infinitesimal distance (Δx). The heat sink is located at a distance $x = (L - \Delta x)$ from the inlet and the acoustic scatterer (array of tubes) is located at $x = L$. The modelling of the heat sink is discussed in the following section. Since the modelling of the acoustic scattering and the derivation of the effective reflection coefficient of the cavity-backed heat exchanger are beyond the scope of our present analysis, the details are not provided in this paper. However, their details can be found in [4, 7]. We only make use of the expression for the effective reflection coefficient i.e.,

$$R_{eff} = R_u + \frac{T_{d\to u}\, T_{u\to d}\, R_p\, e^{2ik_4 l_c}}{1 - R_d\, R_p\, e^{2ik_4 l_c}}, \tag{7}$$

where R and T are the reflection and transmission coefficients, the subscripts u and d denote upstream and downstream characteristics and the subscript p denotes piston, and l_c is the cavity length. $T_{u\to d}$ is the upstream to downstream reflection coefficient, $T_{d\to u}$ is the downstream to upstream transmission coefficient, R_u is the upstream reflection coefficient and R_d is the downstream reflection coefficient. These transmission and reflection coefficients are the elements of the total scattering matrix of the hex which includes the effects of both the heat sink and the acoustic scattering, and they depend on parameters like temperatures and speeds of sound within the resonator, bias flow velocity, geometry of the hex tubes, heat sink properties etc.

3.1 Heat sink

The heat transfer process at the hex can be modelled in two ways: using numerical simulations as shown in Surendran et al. [4], or using an analytical expression like the King's Law or the Heckl correlation [5]. We will use both methods. First we perform numerical simulations to evaluate the heat absorption rate at the hex and subsequently obtain the heat absorption rate law using a transfer function approach. Then we will calculate the heat absorption rate from the Heckl correlation and compare these results with the simulation results.

The heat exchanger transfer function (HTF), which relates the heat absorption rates at the hex to the upstream velocity fluctuations is defined as

$$\mathrm{HTF} = \frac{\hat{Q}_h/\bar{Q}_h}{u/\bar{u}} \,, \tag{8}$$

where $\hat{Q}_h$ and u are the heat absorption rate fluctuation and the upstream velocity fluctuation respectively, in the frequency domain, and $\bar{Q}_h$ and $\bar{u}$ are the corresponding mean quantities. Given the HTF, we can now deduce the $\hat{Q} - u$ relationship from Eq. (8). In analogy to Eqs. (5) and (6), we have the following jump conditions across the heat sink:

continuity of pressure,

$$p_2^+ + p_2^- = p_3^+ + p_3^- \,, \tag{9}$$

and a velocity jump generated by the heat sink,

$$\left(u_3^+ + u_3^-\right) - \left(u_2^+ + u_2^-\right) = \frac{(\gamma - 1)}{S\rho_2 c_2^2}\hat{Q}_h \ . \tag{10}$$

3.1.1 Numerical simulation approach

In the numerical simulation method, the transient heat transfer response of the hex to the incoming velocity fluctuations is obtained using the transfer function approach [8] and a semi-empirical model is derived for the response using a constrained least squares method. Numerical simulations were conducted with the transient CFD solver, ANSYS Fluent 15.0. A 2-D, laminar, incompressible flow was assumed in the domain. Rather than modelling the array of tubes, the computational domain was limited to half of a tube and half of a gap between the tubes, with symmetric boundary conditions on either side. At the inlet and outlet, '*velocity inlet*' and '*pressure outlet*' boundary conditions were imposed, respectively.

In order to apply the transfer function approach, a 'step' perturbation was introduced at the inlet. The total velocity after the step perturbation was $u(t) = \bar{u} + u'$, where $\bar{u}$ is the mean inlet velocity before the step and u' is the magnitude of the step perturbation at the inlet. The resulting heat transfer at the hex was $Q_h(t) = \bar{Q}_h + Q'_h$, where $\bar{Q}_h$ is the mean heat transfer at the hex before the step and Q'_h is the change in the heat transfer due to the velocity change. The transient simulations give the time response of the hex, which is then converted to the frequency response by fast Fourier transform i.e., $u'(t) \xrightarrow{FT} u(\omega)$ and $Q'_h(t) \xrightarrow{FT} \hat{Q}_h(\omega)$.

Figure 2 shows the HTF obtained from numerical simulations for a hex with tubes of diameter (d) 3mm, and a gap of 0.3mm (h_g) between them. The incoming velocity is $\bar{u}$ = 1.0m/s and the amplitude ratios of the velocity fluctuations, $A/\bar{u}$ are 0.05, 0.1, 0.5 and 1.0. From the Fig. 2(a) we can observe that |HTF| exhibits a low pass behaviour and the |HTF| decreases slightly with increasing $A/\bar{u}$ for low frequencies. The phase of the HTF is shown in Fig. 2(b); the curves for the various amplitudes are quite similar for low frequencies, but at higher frequencies, the phase increases with amplitude ratio $A/\bar{u}$.

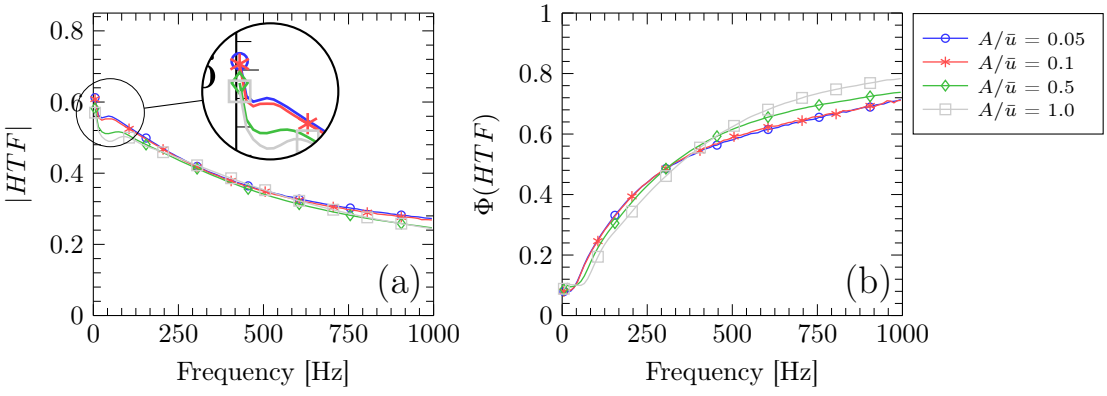

Figure 2: (a) |HTF| and (b) Φ(HTF) obtained from numerical simulations, for d = 3mm, h_g = 0.3mm, $\bar{u}$ = 1.0m/s and different velocity amplitudes.

3.1.2 Heckl correlation

The Heckl correlation [5] can be looked at as a modification to the nonlinear King's law, and it relates the heat transfer rates across a heated wire to the upstream velocity fluctuations. This relation

has been empirically derived and predicts a nonlinear behaviour once the velocity amplitudes exceed about one third of the mean velocity. The Heckl correlation is given by

$$Q(t) = L_w\,(T_w - T)\left\{\kappa + 2\sqrt{\pi\kappa c_v \bar{\rho} d/2}\,\left[\left(1 - \frac{1}{3\sqrt{3}}\right)\sqrt{\bar{u}} + \frac{1}{\sqrt{3}}\sqrt{\left|\frac{\bar{u}}{3} + u'(t-\tau_h)\right|}\right]\right\}, \quad (11)$$

where L_w is the length of the wire, T_w is the temperature of the wire, T is the temperature of the surrounding air, κ is the thermal conductivity of air, c_v is the specific heat of air at constant volume, $\bar{\rho}$ is the mean density, d is the diameter of the wire and $\tau_h = 0.2\ d/\bar{u}$ is the time-lag between the heat transfer and velocity as determined by Lighthill [9]. The HTFs obtained using Eq. (11) in (8)are shown in Fig. 3 for $\bar{u}$ = 1.0m/s. From the Fig. 3(a) we can observe that |HTF| does not exhibit low pass behaviour. It remains almost a constant for the whole frequency range considered. Nevertheless, we can observe that |HTF| decreases with increasing $A/\bar{u}$. The phase plots in Fig. 3(b) all have constant slopes that are equal to τ_h (as expected).

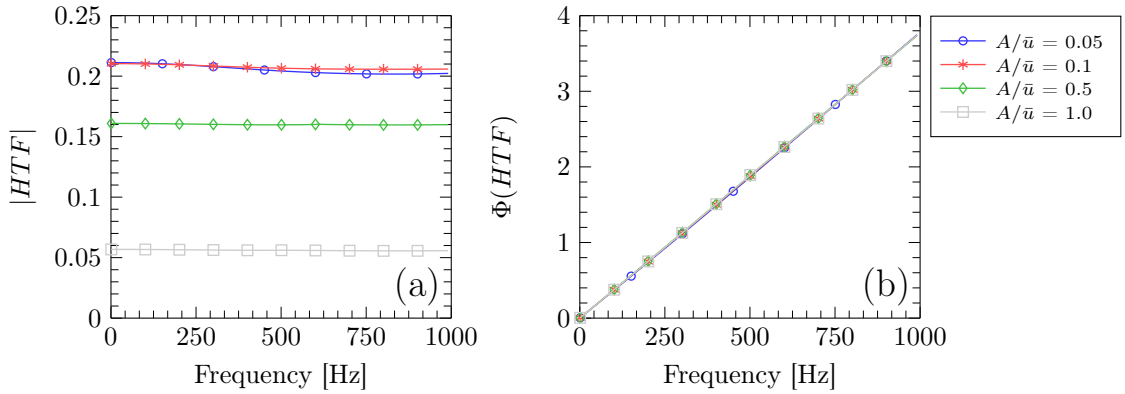

Figure 3: (a) |HTF| and (b) Φ(HTF) obtained from the Heckl correlation, for d = 3mm, h_g = 0.3mm, $\bar{u}$ = 1.0m/s and different velocity amplitudes.

4. Stability Analysis

The combustion system shown in Fig. 1 can now be reduced to that of a duct, open at one end ($x = 0$) and having a reflection coefficient of R_{eff} at the other end ($x = L$). The heat source is located at $x = l_f$. The stability of the combustor is determined using the eigenvalue method [10] and the following conditions are used along with Eqs. (5) and (6) to form the characteristic equation of the system.

At $x = 0$,

$$p_1^+ = R_0\, p_1^- \quad (12)$$

At $x = L$,

$$p_2^- = R_{eff}\, p_2^+ \quad (13)$$

where R_0 and R_{eff} are the reflection coefficients at $x = 0$ and $x = L$ respectively.

Equations (5), (6), (12) and (13) are written as a matrix equation as

$$[Y(\Omega)]\begin{bmatrix} p_1^+ \\ p_1^- \\ p_2^+ \\ p_2^- \end{bmatrix} = \begin{bmatrix} 0 \\ 0 \\ 0 \\ 0 \end{bmatrix}, \quad (14)$$

with matrix

$$[Y(\Omega)] = \begin{bmatrix} e^{-i\frac{\Omega}{c_1}l_f} & -R_0\, e^{i\frac{\Omega}{c_1}l_f} & 0 & 0 \\ 0 & 0 & R_L\, e^{i\frac{\Omega}{c_2}(L-l_f)} & e^{-i\frac{\Omega}{c_2}(L-l_f)} \\ 1 & 1 & -1 & -1 \\ -\left(1+\beta\, e^{i\Omega\tau}\right) & \left(1+\beta\, e^{i\Omega\tau}\right) & \zeta_{12} & -\zeta_{12}. \end{bmatrix}, \tag{15}$$

where $\beta = (n(\gamma-1)) \,/\, (S\rho_1 c_1^2)$ and $\zeta_{12} = (\rho_1 c_1) \,/\, (\rho_2 c_2)$. The characteristic equation, $\det\, Y(\Omega) = 0$, is solved numerically by the Newton-Raphson method or bisection method. The solution, Ω, is a complex quantity of the form $\Omega_m = \omega_m + i\delta_m$, whose real part, ω_m, gives the natural frequency of the mode m, and the imaginary part, δ_m, gives the growth rate. The stability of the mode is determined from the sign of δ_m. Positive δ_m indicates instability and negative δ_m indicates stability.

4.1 System parameters

The combustion system parameters used in our analysis are shown in Table 1.

Table 1: List of system parameters.

Parameter	Notation	Value
Temperature $[K]$	T_1	340
	T_2	1500
	T_4	610
Density $[kg/m^3]$	ρ_1	1.2
Speed of sound $[m/s]$	c_1	341
Duct length $[m]$	L	1
Cross sectional area $[m^2]$	S	0.0025
Cavity length $[m]$	l_c	[0,..,$L/2$]
Heat source location $[m]$	l_f	[0,..,L]
Time-lag law parameters	n $[kg\ m/s^2]$	187
	τ $[s]$	0.15×10^{-3}
Heat exchanger	d $[m]$	0.003
	L_w $[m]$	0.75
	T_w $[K]$	340

4.2 Stability maps

In this analysis, we are interested in the influence of the amplitude of the velocity fluctuations incident on the hex ($A/\bar{u}$), the cavity-length (l_c) and the heat source location (l_f). The stability maps are constructed in the $l_c - l_f$ plane. The *dark* regions indicate instability and the *white* regions indicate stability. Stability of the first mode of the system is determined from the sign of the growth rate, δ_1, as aforementioned.

Figures 4 and 5 show the stability maps obtained from numerical simulations and Heckl correlation respectively. The dashed lines are the boundaries between the stable and unstable regions in subplots (a). From, these results, we can conclude that the amplitude of the velocity fluctuations are

very important in determining the stability of the combustion system. Here, an increase in $A/\bar{u}$ tends to destabilise the system. This trend is exhibited by both models, albeit rather more strongly for the Heckl correlation.

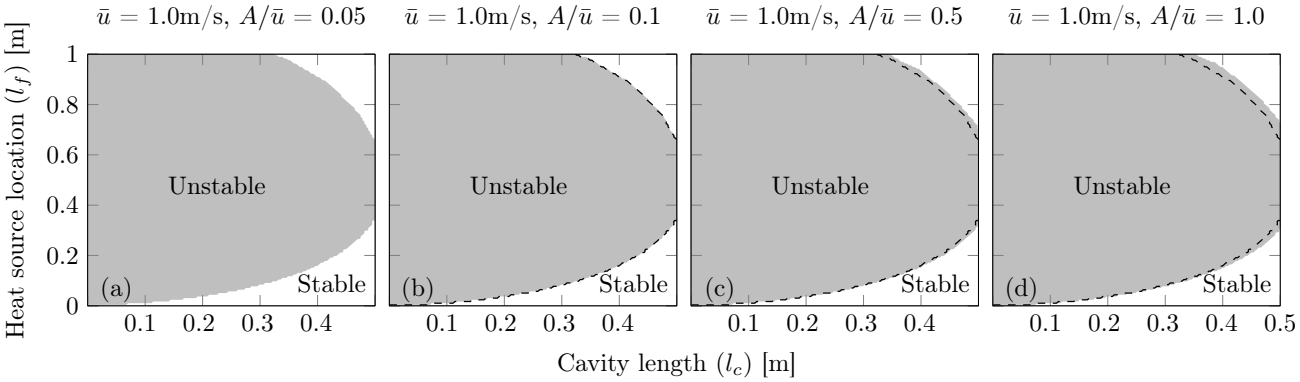

Figure 4: Stability maps for d = 3mm, h_g = 0.3mm, $\bar{u}$ = 1.0m/s and (a) $A/\bar{u}$ = 0.05, (b) $A/\bar{u}$ = 0.1 (c) $A/\bar{u}$ = 0.5 and (d) $A/\bar{u}$ = 1.0, from numerical simulations.

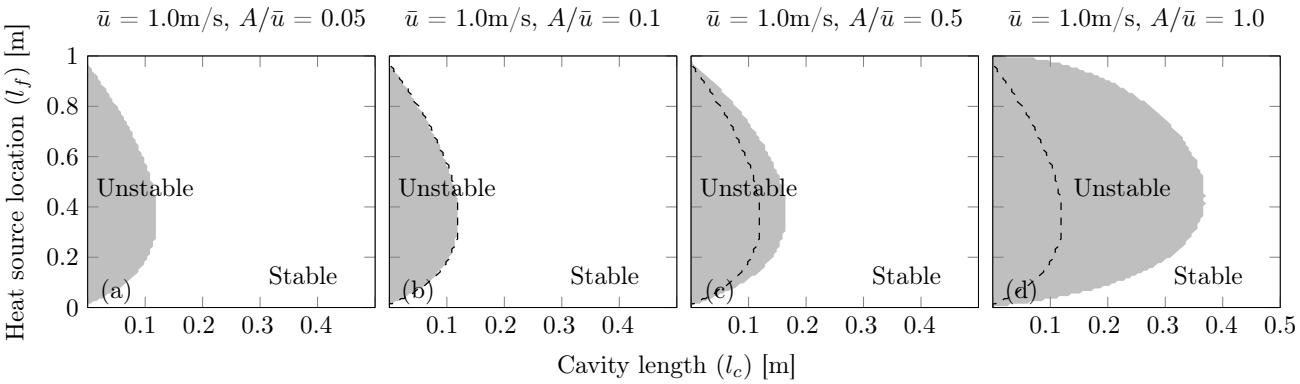

Figure 5: Stability maps for d = 3mm, h_g = 0.3mm, $\bar{u}$ = 1.0m/s and (a) $A/\bar{u}$ = 0.05, (b) $A/\bar{u}$ = 0.1 (c) $A/\bar{u}$ = 0.5 and (d) $A/\bar{u}$ = 1.0, from Heckl correlation.

5. Conclusion and Outlook

Stability analysis was conducted on a quarter-wave resonator including a heat source and a heat exchanger near the downstream closed end. The heat sink was modelled using two approaches: numerical simulation approach and an analytical approach. The key parameter in the stability predictions is the amplitude of the velocity fluctuations upstream of the heat exchanger. We observe that an increase in the amplitude of the velocity fluctuations tend to destabilise the system. This trend is observed in both numerical as well as analytical calculations. An initial interpretation, which will need to be confirmed, is that hex tubes become less effective as a heat sink as the amplitude increases. Presently, work is in progress to analyse this system in detail and to fully understand the effect of the amplitude of the velocity fluctuations.

Acknowledgements

The presented work is part of the Marie Curie Initial Training Network Thermo-acoustic and Aero-acoustic Nonlinearities in Green combustors with Orifice structures (TANGO). We gratefully

acknowledge the financial support from the European Commission under call FP7-PEOPLE-ITN-2012.

REFERENCES

1. Lord Rayleigh, *The Theory of Sound*, vol. II, Dover Publications, 2nd edn. (1896).
2. Riess, P. Das Anblasen offener Röhren durch eine Flamme, *Annalen der Physik und Chemie*, **184**, 653–656, (1859).
3. Surendran, A. and Heckl, M. A. Passive instability control by using a heat exchanger as acoustic sink, *The 22nd International Congress on Sound and Vibration*, Florence, Italy, 12–16, July, (2015).
4. Surendran, A., Heckl, M. A., Hosseini, N. and Teerling, O. J. Use of heat exchanger for passive control of combustion instabilities, *The 23rd International Congress on Sound and Vibration*, Athens, Greece, 10–14, July, (2016).
5. Heckl, M. A. Non-linear Acoustic Effects in the Rijke Tube, *Acustica*, **72** (1), 63–71, (1990).
6. Heckl, M. A. Active control of the noise from a Rijke tube, *Journal of Sound and Vibration*, **124** (1), 117–133, (1988).
7. Surendran, A., Passive control of thermoacoustic instabilities in idealised combustion systems using heat exchangers, PhD Thesis, Keele University, Submitted, (2017).
8. Hosseini, N., Kornilov, V., Teerling, O. J., Lopez Arteaga, I. and de Goey, L. P. H. Transfer function calculations of segregated elements in a simplified slit burner with heat exchanger, *The 22nd International Congress on Sound and Vibration*, Florence, Italy, 12–16, July, (2015).
9. Lighthill, M. J. The response of laminar skin friction and heat transfer to fluctuations in the stream velocity, *Proceedings of the Royal Society A: Mathematical, Physical and Engineering Sciences*, **224** (1156), 1–23, (1954).
10. Heckl, M. A., *Heat Sources in Acoustic Resonators*, Ph.D. thesis, Emmanuel College, University of Cambridge, (1985).